Geo-Marine Letters (2021) 41: 33
https://doi.org/10.1007/s00367-021-00708-5

ORIGINAL

Large scale excavation of outer shelf sediments by bottom currents during the Late Miocene in the SE Atlantic

Andrew Hopkins[1,2] · **Joe Cartwright**[3]

Received: 9 February 2021 / Accepted: 16 June 2021 / Published online: 9 July 2021

Abstract

An unusual erosional surface has been identified on seismic data from the outer shelf on the northern Namibian margin. The undulating surface defines a depression extending for 1300 km^2 from which fine-grained Miocene sediments have been excavated to a depth of up to 160 m. The depression has a kidney-shaped planform, with three deep pits marking its basinward extent. It is an entirely closed feature, with no evident channels feeding in or leading out. Subsequent sedimentation has completely filled in the depression with the earliest infilling units exhibiting unusual depositional geometries. Well correlation yields a date of 9.9 ± 1.0 Ma for the erosional surface. No analogous features are known, but of all the possible causal mechanisms, it is considered most likely that the erosional depression was created by the extraordinary action of eddying bottom currents. These were probably associated with the well-documented Late Miocene onset of intensification of the Benguela Upwelling System, and were possibly directed by a small local variation in sea bed relief.

Introduction

The growing body of literature examining the products and processes attributable to the action of marine bottom currents is dominated by examples from continental slopes and from basin floors. (e.g. Rebesco et al. 2014). Far fewer cases have been reported from continental shelf environments, a bias that can be explained by the fact that the global thermohaline system tends to operate at depths below several hundred metres. The relatively uncommon sediment drifts and erosional features that do occur on continental shelves are generally attributed to more localised current regimes. They can however be significant in scale (e.g. Fulthorpe and Carter 1991; Verdicchio and Trincardi 2008) and they have possible implications for aspects of petroleum geology. For example, they may be important for understanding the impact of shallow-water bottom currents on shelf anoxia, on the reworking and distribution of shelf reservoirs and on the delivery of shelfal sands to deeper water environments.

In this paper, we discuss the interpretation of a 2D seismic dataset from the northern Namibian continental margin (Figs. 1 and 2). Within the dataset, we have identified a highly unusual morphological depression with an areal extent of 1300 km^2 and up to 160 m of relief (Fig. 3). This large depression is hosted in sediments deposited on the palaeo-shelf during the Neogene. It is therefore presumed to have formed under shallow bathymetric conditions. However, unlike all other major erosional features that are known to form in shelf environments such as incised valleys or submarine canyons, this feature has a closed perimeter, i.e. it does not open into the deeper water but is entirely enclosed on all its lateral margins. Superficially, it thus resembles a large crater, and we consider a range of possible known crater-forming mechanism such as caldera collapse (e.g. Branney 1995), bolide impact (e.g. Stewart 2003) and focused fluid expulsion (e.g. Cartwright and Santamarina 2015). Also, by analysing the external morphology, truncation geometry and disposition of the sedimentary infill, we consider the possibility that this feature was caused by intensive vertical eddying in shelfal water depths off the coast of Namibia, during the Late Miocene. Contemporary eddy systems are well known from this part of the South Atlantic (e.g. Clement and Gordon 1995; Penduff et al. 2001), and we draw on modern analogues in weighing up this possible

✉ Andrew Hopkins
andrew.hopkins@ucl.ac.uk

[1] School of Earth and Ocean Sciences, Cardiff University, Cardiff CF10 3AT, UK

[2] Department of Science and Technology Studies, University College London, London WC1E 6BT, UK

[3] Department of Earth Sciences, University of Oxford, Oxford OX1 3AN, UK

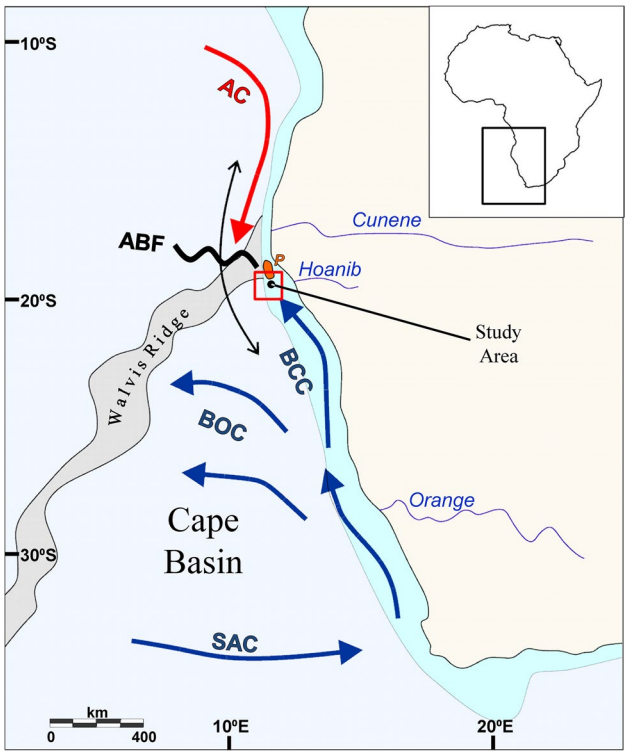

Fig. 1 Regional setting showing the Benguela Upwelling System in the Cape Basin: South Atlantic Current (SAC), Current Benguela Coastal Current (BCC), Benguela Oceanic Current (BOC), Angola Current (AC) and Angola-Benguela Front (ABF – along-coast movement shown by the black two-headed arrow). After Jansen et al. 1996. *P* marks the site of the buried Phoenix volcano (Corner et al. 2002)

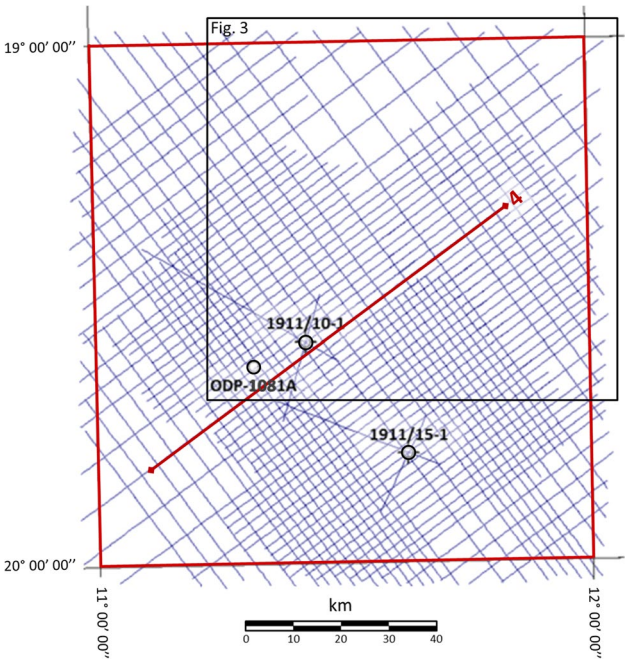

Fig. 2 Base map for seismic profiles and boreholes. The area covered by Fig. 3 and the location of Fig. 4 are also shown

explanation. If correct, this would be the first such description of large scale erosion by a major oceanic eddy system on a continental shelf in the stratigraphic record, with concomitant implications for the interpretation of shelf systems in a wider sense.

Regional geological setting

Modern physiographic setting

The study area is located about 60 km offshore at the northern end of the present-day Cape Basin (Fig. 1). It covers part of the southern flank of the aseismic Walvis Ridge, which separates the Cape Basin from the Angola Basin to the north, and which runs from its coastal abutment for 2500 km towards the Mid Atlantic Ridge. It forms a barrier to northward and southward flow below a water depth of about 3000 m (Shannon 1985) and thus exerts a major influence on deep circulation in the southeast Atlantic. The present-day continental shelf along this part of the Namibian margin is unusually wide at about 40 km, with a relatively broad and upwardly convex shelf-slope break. The water depth at the shelf break as measured on seismic data ranges from 350 to 400 m, which is unusually deep by global norms (Van Andel and Calvert 1971).

Geological evolution

Recent studies place the onset of sea-floor spreading in the southernmost Atlantic within the Valanginian (Perez-Diaz and Eagles 2014: 138 Ma; Hall et al. 2018: 135 Ma). Plate reconstructions point to a northward opening of the South Atlantic, such that break-up took place sequentially across a series of segment boundaries aligned perpendicular to the margin (Heine et al. 2013). The part of the margin immediately south of the Walvis Ridge (known as the Walvis Basin, e.g. Light et al. 1993), underwent an initial period of extensional faulting in the late Albian. Subsequently, a predominantly clastic depositional system became established, infilling the rifted topography, and superseding a succession of pre-rift platform carbonates (Holtar and Forsberg 2000). At the northern end of the Walvis Basin, a major submarine volcanic centre, the Phoenix High (*P* in Fig. 1), was emplaced on the south side of the Walvis Ridge in Cenomanian to Turonian times (Corner et al. 2002) and was subsequently buried by later sediment. Drilling results indicate that the post-rift succession is mud-dominated, and is punctuated only rarely by sandy turbiditic flows (Holtar and Forsberg 2000). The Angolan margin to the north of the Walvis Ridge experienced major uplift and rotation during the Miocene (Jackson et al. 2005). However, there is no evidence of significant tectonic or gravity-driven deformation

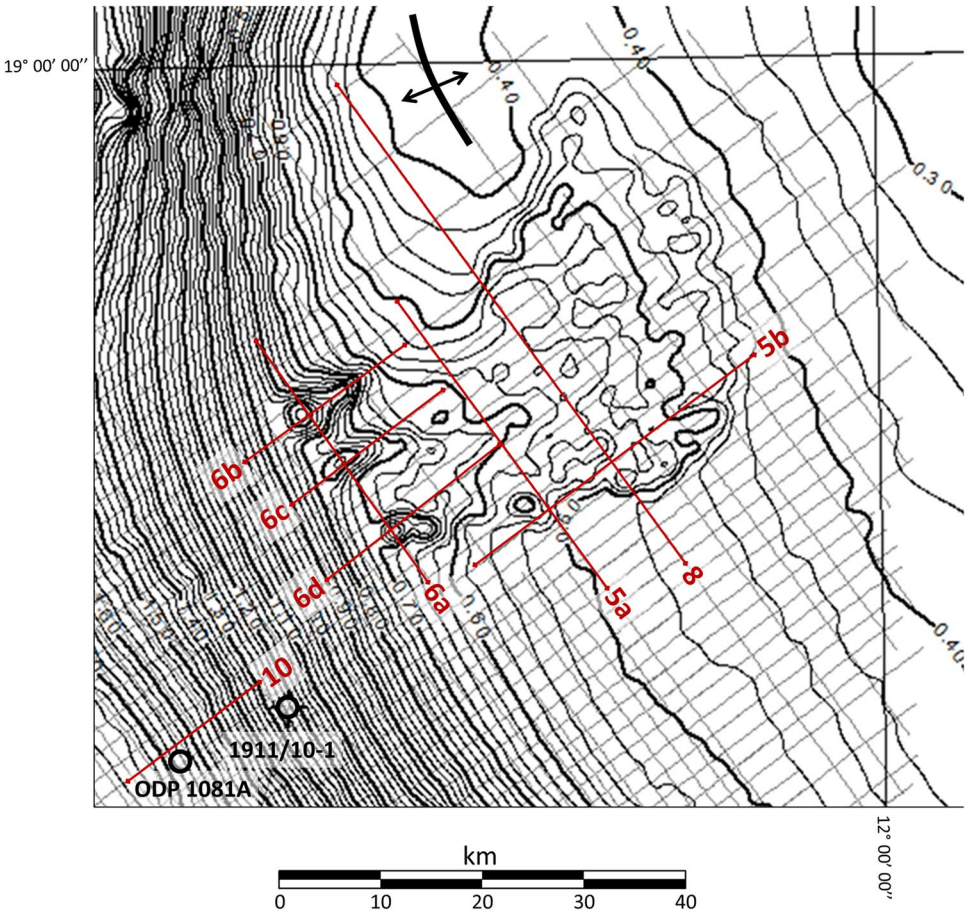

Fig. 3 Two-way travel time contour map of the erosion surface and the surrounding correlative conformity surface (contour interval = 0.025 s TWTT (25 ms)), with locations of Figs. 5, 6, 8 and 10

at any time during the Neogene, the main interval of interest for this study, in the basins to the south.

Neogene stratigraphy and palaeoceanography

ODP and DSDP wells (from Sites 352 and 1081 respectively) provide valuable information on lithostratigraphy (Diester Haass et al. 1990; Pufahl et al. 1998). The Neogene sedimentary succession comprises almost entirely hemipelagic muds, clays and calcareous oozes, with a significant biogenic component, reflecting the paucity of land-derived material due to the aridity of the adjacent onshore areas (Aizawa et al. 2000). The biogenic components demonstrate the high productivity of the margin, which is one of the world's most prolific upwelling systems. Evidence from palaeoproductivity proxies, together with other studies of regional oceanography and onshore geology, indicates that cold water has been upwelling along the Namibian margin since ca. 10 Ma (Siesser 1980; Rommerskirchen et al. 2011). Upwelling started in response to the intensification of the Benguela Upwelling System (BUS, Fig. 1), which had been active in a weak form since ca. 14 Ma (Diester Haass et al. 1990). Onshore, in response to the strengthening BUS, the existing semi-arid conditions were intensified leading to the interior becoming hyper-arid. Landscapes were stabilised with the development of pedogenic calcretes (Ward and Corbett 1990), further limiting erosion.

The two main near-shore components of the BUS are the cold, northward flowing Benguela Current (BC), and the Angola Current (AC), which brings warm, tropical water southward (Fig. 1). The coastal branch of the BC, the Benguela Coastal Current (BCC) and the AC converge at the Angola-Benguela Front (ABF), a line roughly perpendicular to the margin, to create a zone of strong current activity and eddying (Lass et al. 2000). The ABF has moved northwards and southwards along the Angolan-Namibian margin during its existence in response to changes in hydrography and wind stress (Jansen et al. 1996).

Database and methods

Seismic data

The study is based on the interpretation of 7900 line kilometres of time-migrated seismic reflection profiles (Fig. 2). These were acquired during petroleum exploration campaigns in the 1990s (Holtar and Forsberg 2000), and the

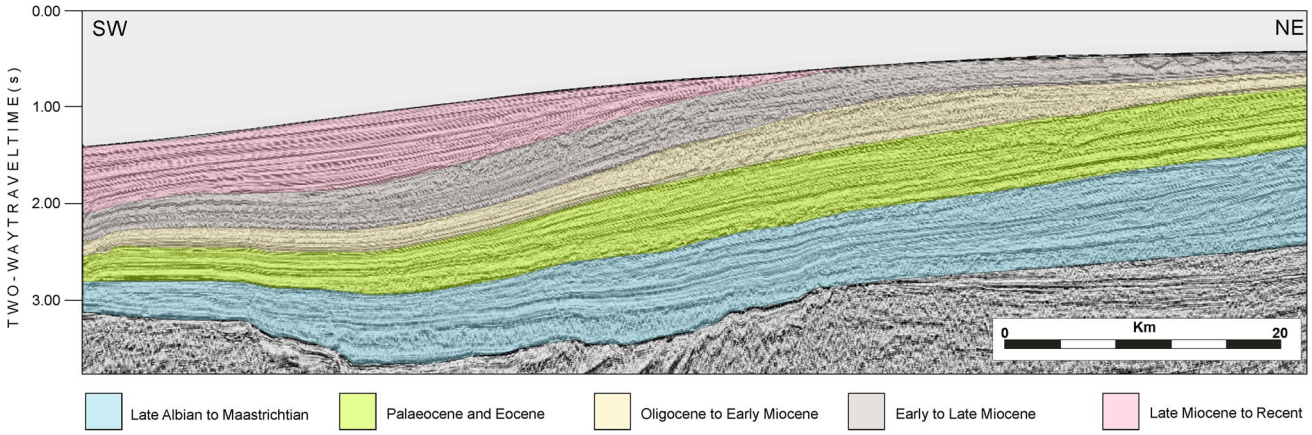

Fig. 4 Regional seismic profile (dip orientation) showing the major post-rift tectono-stratigraphic units of the Walvis Basin. The erosional surface that forms the depression is evident immediately below the seabed reflection at the top right of the Fig. See Fig. 2 for location

study area, which is bounded by the red outline on Fig. 2, corresponds to Licence Block 1911. This high-resolution multichannel dataset is arranged orthogonally with lines spaced between 2 and 8 km apart. Reflections within the interval spanning the erosion surface and its infill have resolution limits of ca. 15 m vertically and ca. 25 m laterally. These limits are based on a dominant frequency of 60 Hz and assume average P-wave interval velocity of 1600 m/s (for poorly consolidated shelf sediments), and are calculated using standard formulations (Sheriff 1977). Data quality is generally excellent with a high signal-to-noise ratio. The zone of interest is too shallow to be affected by sea-bed multiples, though some short period reverberations are evident (see "Seismic interpretation of the erosion surface" section).

Two deep oil exploration boreholes (1911/10–1 and 1911/15–1) and ODP well 1081A are situated within 40 km of the basinward side of the feature (Figs. 2 and 3). All three intersect the seismic grid and provide valuable stratigraphic calibration. Standard seismic-stratigraphic interpretation techniques were used to identify and correlate prominent stratigraphic surfaces, including the major erosional surface that forms the focus of this study (Mitchum et al. 1977; Brown and Fisher 1977). Geoframe and IHS Markit Kingdom software were used for digital seismic interpretation. Individual horizons were, however, picked manually following accepted principles rather than by automatic tracking correlation (e.g. Ashcroft 2011).

Results

Seismic stratigraphy

The seismic stratigraphy of the Walvis Basin has been divided by previous authors into major "geometrically confined " tectono-stratigraphic units (Holtar and Forsberg 2000; see also e.g. Light et al. 1993). The post-rift units highlighted in Fig. 4 (see Fig. 2 for location) broadly correspond to the "W" prefixed sub-divisions of Holtar and Forsberg (2000) as follows: Late Albian to Maastrichtian: W3 to W5; Palaeocene and Eocene: W6-1 to W6-4; Oligocene to Early Miocene: W6-5; Early to Late Miocene: W6-5 to W6-6; Late Miocene to Recent: W7.

All of the post-rift units consist of mainly fine-grained sediments. The seismic configurations of the pre-Early Miocene units are dominantly progradational/aggradational. The Early to Late Miocene unit however is characterised by a much more aggradational stacking configuration on both the shelf and the slope (Aizawa et al. 2000). The youngest, Late Miocene to Recent seismic-stratigraphic unit onlaps against the outer shelf break and is notably absent (or considerably condensed) on the modern shelf. Our main focus is on the Early to Late Miocene unit on the shelf, which is characterised by laterally continuous reflections that provide excellent constraints for regional chrono-stratigraphic correlation (Fig. 4).

Seismic interpretation of the erosion surface

The erosional nature of the surface is evident from the systematic truncation of underlying stratal reflections in the centre of the study area. Using standard interpretation techniques (Vail et al. 1977; Emery and Myers 1996), the highly undulating erosion surface can be interpreted on 17 dip lines and 7 strike lines as a prominent seismic reflection generally occurring within 150 ms (TWTT or ca. 120 m) of the present day sea-floor. The depression formed by the erosion surface corresponds to the envelope of truncated reflection terminations (Figs. 5 and 6). Truncation geometries are pronounced, often with relatively large angles of

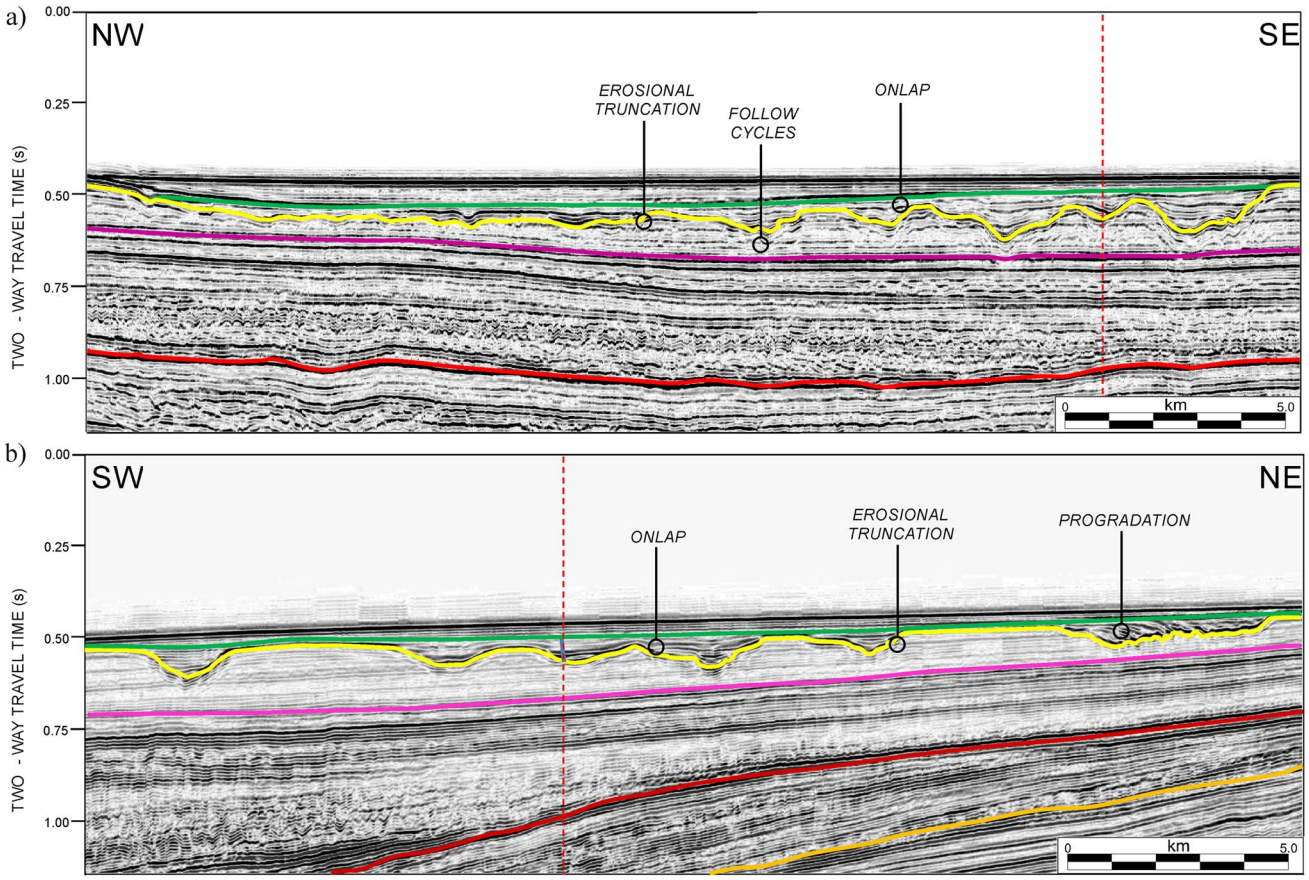

Fig. 5 Representative strike (**a**) and dip (**b**) oriented profiles across the erosional depression. Intersection shown as dashed red line. Horizons shown are: Near Top Palaeocene (orange); Near Top Eocene (red); Near Top Early Miocene (magenta); Late Miocene erosional surface (yellow); top of lower infilling unit M1 (green). Examples of key reflection characteristics are highlighted. See Fig. 3 for locations

up to 12° (e.g. Figure 6d), which are classically typical of erosional processes that involve localised excavation of the substrate or down-cutting (Brown and Fisher 1977; Emery and Myers 1996). The infilling sediments exhibit onlapping and downlapping reflection configurations at the margins of the erosional depression (Figs. 5 and 6).

The erosion surface occurs in continuous segments and is readily identifiable, especially where truncation is angular (see examples of erosional truncation in Figs. 5 and 6). Generally, the surface produces a high amplitude positive or 'hard' reflection signifying an increase in acoustic impedance. Amplitude, phase and polarity do however vary somewhat as the acoustic properties of the lithologies juxtaposed above and below the erosion surface vary. The unambiguous truncation geometry of the reflection is however occasionally obscured by short period reverberations (follow cycles, e.g. Figure 5a), and by the low frequency water bottom reflection. The spacing of the dip lines is considered adequate to avoid significant spatial aliasing (Emery and Myers 1996).

Laterally, the erosion surface passes into a concordant package of reflections as a correlative conformity (sensu lato, e.g. Figure 6d). However, some of the correlative reflections do not quite tie consistently at line intersections which may indicate a degree of diachroneity. Alternatively, the minor mistie problem may simply be due to the intrinsic limit of vertical resolvability at the lateral margin of the erosion surface.

Morphology of the erosion surface

The erosion surface has a planform that is roughly kidney shaped, measuring approximately 40 by 50 km with a slight elongation orthogonal to the coastline, i.e. in a NE-SW direction (Fig. 3). Importantly for any consideration of the origins of this erosional feature, the mapped positions of its margins reveal it to be entirely enclosed. That is, it does not open out anywhere into another erosional feature, but is completely surrounded by conformable reflection configurations. No channels feeding into the erosional feature from the palaeo-coastline are evident (Fig. 3).

A 3D visualisation of the erosional feature constructed from the gridded interpretation (Fig. 7) shows the depression

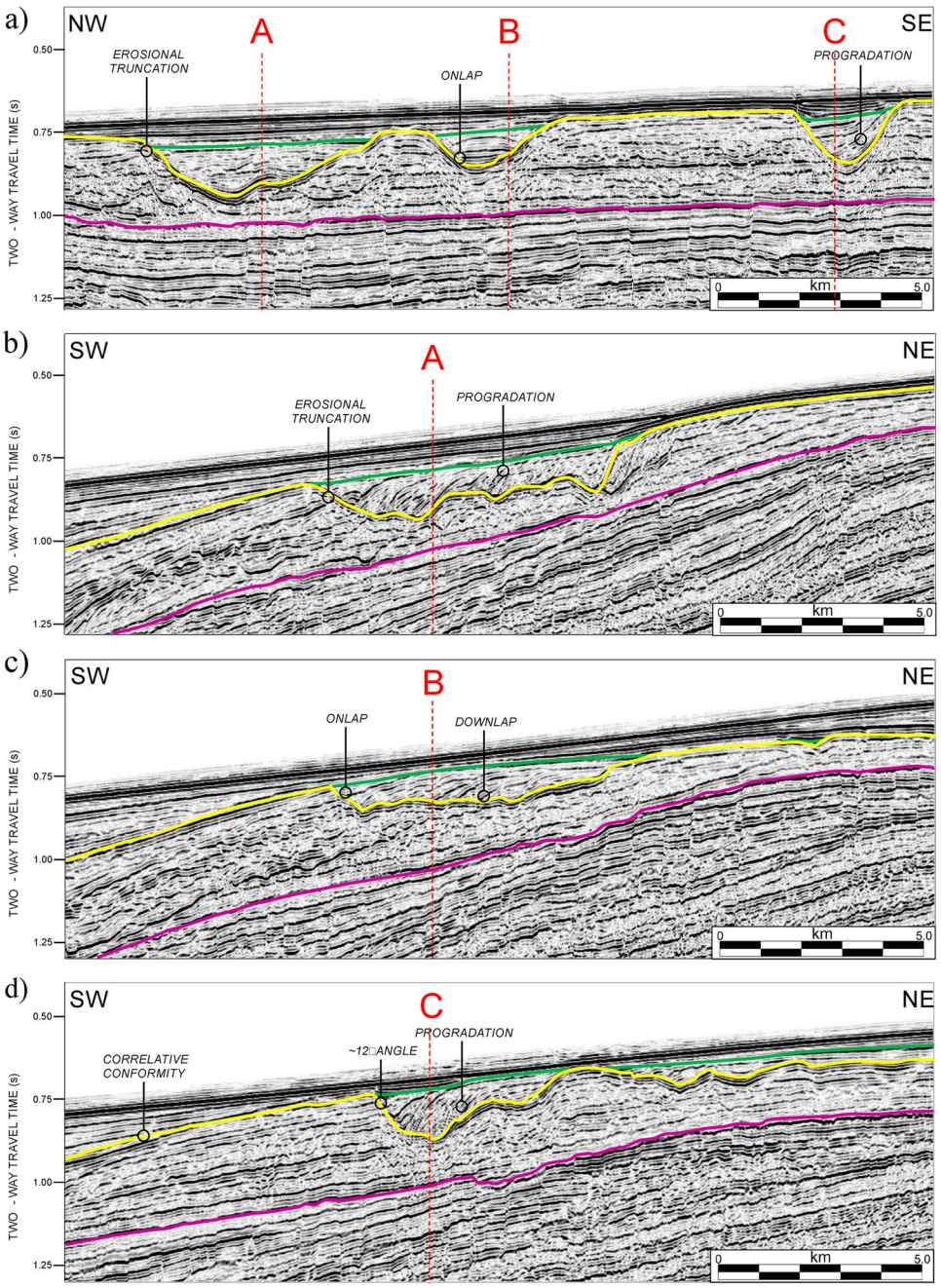

Fig. 6 Seismic profiles across deep pits, A, B and C in strike orientation (**a**) and dip orientation (**b**), (**c**) and (**d**); intersections marked with red dashed vertical lines. Faults omitted for clarity. Horizons shown are: Near Top Early Miocene (magenta); Late Miocene erosional surface (yellow); top of lower infilling unit M1 (green). Examples of key reflection characteristics are highlighted. See Fig. 3 for locations

wrapping around the southern and south-eastern sides of a low relief topographic mound (the high axis in Fig. 3). This is the remnant expression at the sea floor of the buried Late Cretaceous Phoenix High volcanic centre ("*P*" in Figs. 1 and 8; see also Fig. 14 in Holtar and Forsberg 2000).

The morphology of the erosion surface is illustrated by two representative seismic profiles (Figs. 5a and b). On dip profiles, the surface forms a series of undulating, quasi sinusoidal highs and lows, with the relief on the surface generally increasing basinward (Fig. 5b). The irregular relief is also evident on strike orientations, though the profile is more asymmetrical, with the slope of the excavated surface being markedly more gentle to the north-west than on the south-eastern side (Fig. 5a).

Internally, the depression consists of three curved, subparallel troughs with two intervening ridges (Figs. 3 and 7). The outermost of these troughs defines the eastern boundary of the depression and curves in strike through nearly 90°, from NW–SE inshore, to SW-NE at the basinward margin. The outer edge of the depression has an angular, clearly defined lip on seismic profiles, with no evidence of levees or marginal build-ups (Figs. 5 and 6). The two inner troughs are

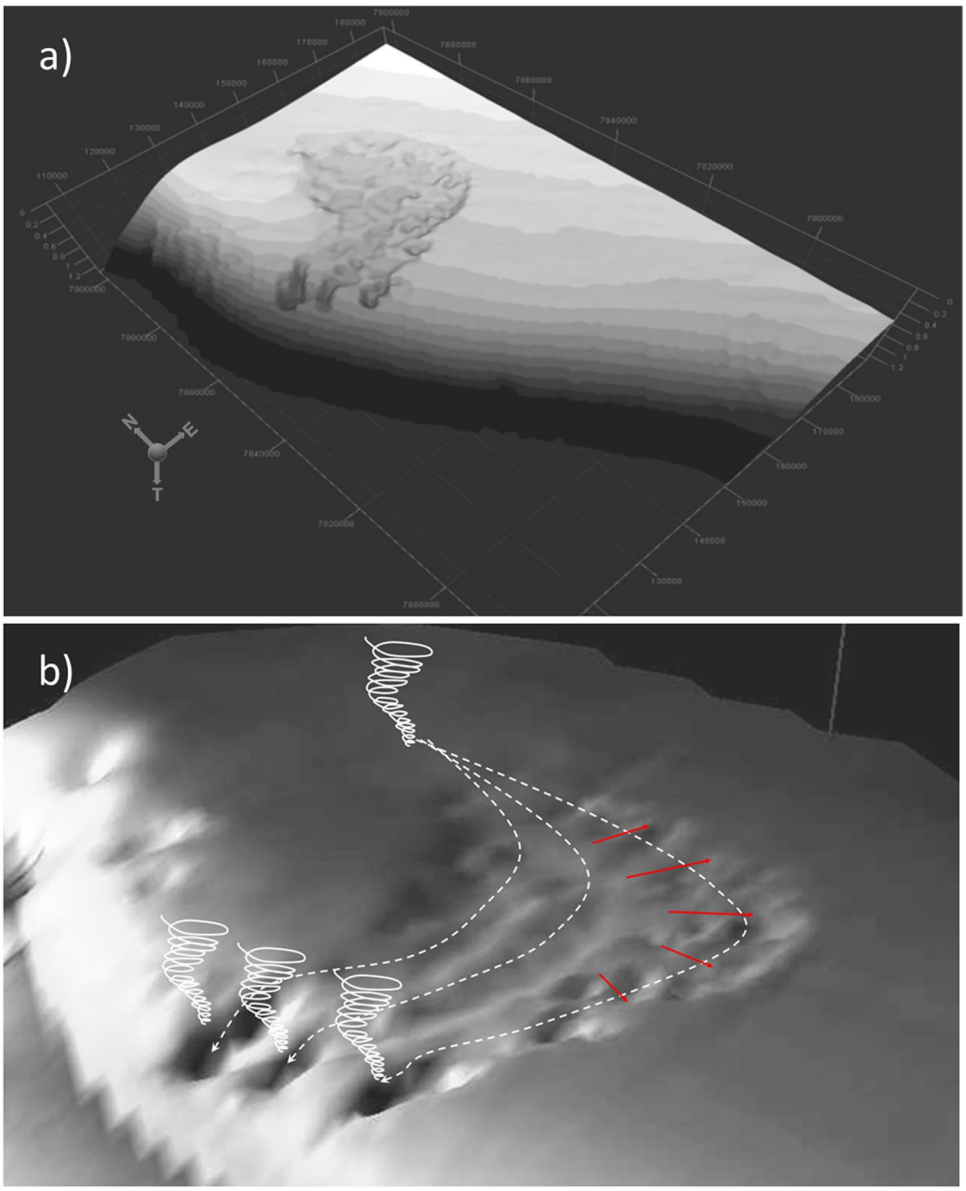

Fig. 7 **a** Three-dimensional rendering of erosional depression and surrounding correlative conformity surface. Horizontal axes: 120 × 80 km; vertical axis: 1.2 s TWTT; (**b**) Close-up 3D view of erosional depression looking to the NNE showing the suggested path of erosive eddies. Red arrows indicate intensification of erosion and direction of subsequent downlapping sedimentation around outer edge

shorter and much less curved, and are encompassed by the arc of the long outer trough. All three troughs become less well defined towards the north-western end of the depression, which tapers to a point. The three troughs merge here and level off into a broad, relatively flat area (Figs. 3 and 7).

On the basinward side of the erosional depression, each of the three troughs shallows before plunging down into a deep, terminal pit (Figs. 3 and 7). These three pits (A, B and C on Fig. 6) are perhaps the most striking features of the entire erosional depression, and appear to represent loci of maximum down-cutting. There is no common datum (base level) for the depth of erosion either beneath the modern seabed or beneath a datum interpolated from the marginal correlative conformities surrounding the feature. There is therefore no geometrical indication that the depths of the deepest portions of the erosion surface relate to any form of regional base level under any definition of that term (e.g. Schumm 1993; Catuneanu 2003).

The three pits are all broadly elliptical in map view. Each forms a fully enclosed low of the order of 8 km in length and 3–4 km in width, with an erosional relief of 100–160 m. All three are relatively symmetrical in their short axis orientation (Fig. 6a), though each has an asymmetric longitudinal section (Figs. 6b, c and d), with the steeper dip occurring on the basinward side. The steepest slope associated with the entire erosional depression occurs on the south-west side of pit C, which dips at approximately 12° to the northwest (Fig. 6d).

Each of the elliptical pits is marked by a lip that defines the basinward limit of each trough (Figs. 6 and 7b). They

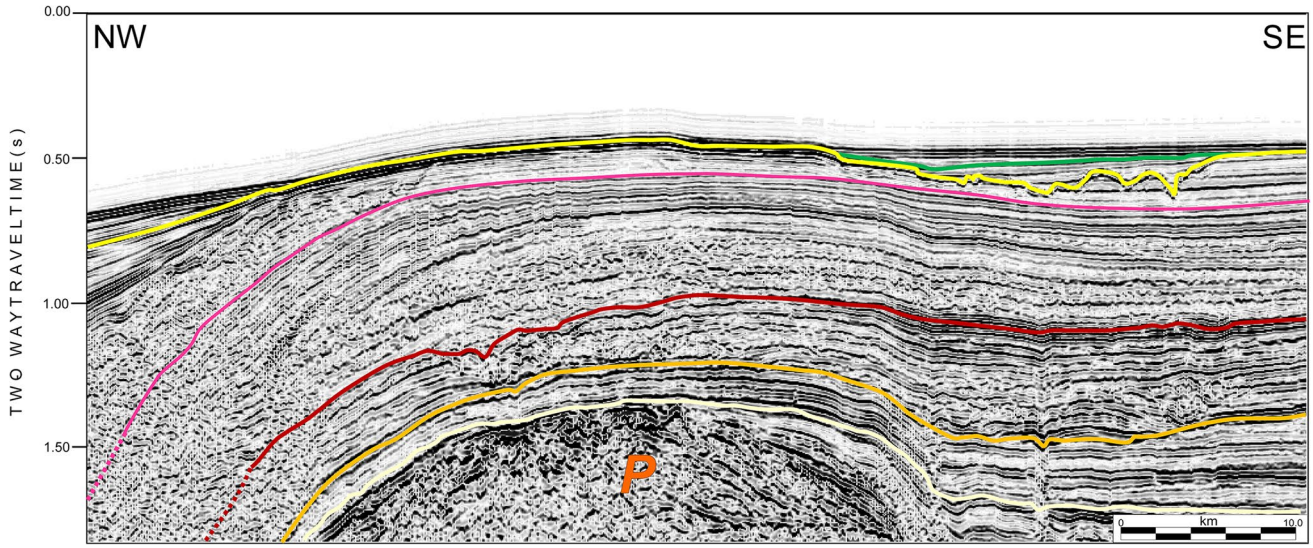

Fig. 8 Seismic profile across the buried Turonian-Cenomanian Phoenix volcanic edifice (*P*). Horizons shown are: Base Cenozoic (beige); Near Top Palaeocene (orange); Near Top Eocene (red); Near Top Early Miocene (magenta); Late Miocene erosional surface (yellow); top of lower infilling unit (green). Note the influence that Phoenix continues to exert on present-day sea bed topography, and the location of the erosional depression with respect to the sea floor bulge. See Fig. 3 for locations

step progressively basinward by several kilometres relative to strike from southeast to northwest (Figs. 3 and 7b), though all three pits terminate on the upper palaeo-slope as judged by their positions relative to palaeo-slope breaks on clinoform surfaces (see "Palaeo-water depth" section). There is no evidence that the process that eroded the depression was active basinward on the surface of the palaeo-slope, which is undisturbed at a seismic scale, and exhibits uniformly concordant reflection geometries.

Subcrop relationships

The erosion surface appears to have cut downwards into the pre-existing strata at random. That is, the erosive process does not appear to have exploited any inhomogeneity or weakness in the underlying stratigraphy or structure. The stratal configurations of the eroded units are parallel, conformable and sub-horizontal consistent with their interpretation as former shelf deposits (Figs. 5 and 6).

Palaeo-water depth

The transitional form of the shelf-slope system, with no clear clinoform breakpoints (Fig. 4), makes it difficult to determine palaeo-water depths. This is consistent with the conclusion that terrigenous input has been severely limited throughout much of the Neogene (Pufahl et al. 1998; Aizawa et al. 2000).

At several points along the margin, small shelf delta systems have been preserved at the present day sea floor, and these provide the means to estimate palaeo-sea level (Fig. 9). The topsets present at the sea floor currently lie

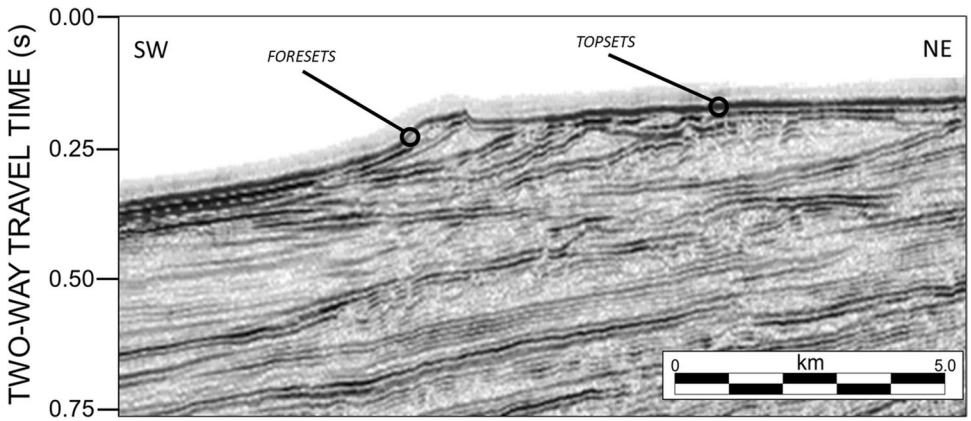

Fig. 9 Example of shelf delta, approximately 150 km along the shelf to the southeast of the study area, used to estimate palaeo-water depth

in about 130 m of water but would have been at or very close to sea level at the time of deposition. Assuming that present day sea level includes a post-glacial rise of 120 m since the Pleistocene (Gornitz 2009), the net relative sea level rise is ca. 10 m. The topsets of the shelf delta system include the extrapolation of the reflection forming the correlative conformity as interpreted on the south side of the erosional feature which can therefore be regarded as a time-equivalent surface. If depths to the uneroded margins of the depression are approximately 340 m at the present day, then water depths at the onset of erosion were about 330 m. The present-day topset surface is approximately horizontal, so it is assumed that there has been negligible basinward rotation and no appreciable along-strike tilting since the time that this major erosional episode took place. Differences in compaction along the dip profile can also reasonably be assumed to be negligible, and this palaeo-water depth estimate of 330 m can therefore be taken as a valid approximation.

Sedimentary infill – reflection configuration

The sediments infilling the eroded depression can be subdivided into two informal seismic stratigraphic units (M1 and M2), based on their distinctive seismic facies and reflection configurations (Figs. 5 and 6).

Unit M1

The lower unit comprises reflections that exhibit variable internal configurations and relationships to the underlying erosion surface. These configurations include onlap, drape and bi-directional downlap (Figs. 5 and 6). Reflection patterns include both parallel and divergent relationships. Most notably however, reflections in the lower unit downlap the erosion surface and prograde towards the eastern and south-eastern margins of the excavation (Fig. 5b). Downlap is particularly evident against the relatively steep sides on the outer curve of the outer trough, where the direction of progradation and downlap rotates so that it remains approximately perpendicular to the margin of the depression (see arrows in Fig. 7b). In the three elliptical pits (A, B and C of Fig. 6) however, where downlap occurs, the direction is exclusively basinward (Figs. 6b, c and d).

A strike profile across the three elliptical pits (Fig. 6a) illustrates some of the variety of reflection configurations in the lower unit. The lowermost reflections in pit A lie subparallel to the underlying erosion surface, and onlap or gently downlap the sides. Overlying, low amplitude reflections are mainly parallel and sub-horizontal, but with indications of divergence on the south side. In pit B, the lowermost reflections are sub-horizontal and parallel. The subsequent two or three cycles however, display bi-directional downlap. On the south flank of pit C, infilling reflections lie in a prograding, sigmoid configuration. This pattern is reminiscent of the lateral accretion that commonly occurs in submarine channel environments (Wonham et al. 2000; Abreu et al. 2003), suggesting that a similar process of axial flow that shifts progressively laterally may have been operative during erosion and deposition. Overlying strata are represented by sub-horizontal reflections indicating the change to a more aggradational style of deposition.

Unit M1 reaches a maximum thickness of up to 130 m in the elliptical pits. In the main part of the erosional depression, it thickens to the southeast, towards the outer curved margin (Fig. 5a). The surface marking the top of the lower unit just fails to cover all of the more prominent highs within the depression, and dips gently basinward (Figs. 5 and 6).

Unit M2

Unit M2, seen overlying the green horizon in Figs. 5 and 6, is characterised by sub-horizontal, parallel reflections, which are generally more continuous and have stronger amplitudes than those of the lower unit. Reflections in this unit tend to be obscured by low amplitude multiples from the sea floor. Its thickness is greatest over the central parts of the erosional feature, reaching about 70 m, thinning to below seismic resolution around the margins.

The present seafloor exhibits no vestiges of the earlier episode of erosion, the feature having been completely filled by the two units described, and by subsequent pelagic/hemipelagic deposition. The Phoenix High however, has a continuing low relief expression at the seafloor today (Fig. 8 and see structural high axis in Fig. 2).

Timing of the erosional episode

The erosion surface was dated by tying the correlative conformity to the most reliably dated nearby well. Of the three wells in the study area, only ODP 1081A (Pufahl et al. 1998) was able to provide viable constraints on age dating from biostratigraphy (Fig. 10). This borehole reached its total drilled depth 38 ms or approximately 35 m[1] above the correlative conformity surface, so extrapolation using average sedimentation rates was required to derive a probable age for the correlative conformity, and hence to enable the end of the hiatus corresponding to the erosional episode to be bracketed.

[1] An interval velocity of 1850 m/s was derived from check shots in the exploration wells 1911/10–1 and 1911/15–1 for Miocene sediments on the continental slope, giving a depth interval of 35 m. This interval velocity has been used in preference to the unrealistic value of 1500 m/s which Wefer et al (1998) assumed for the entire section between the seafloor and the bottom of the hole.

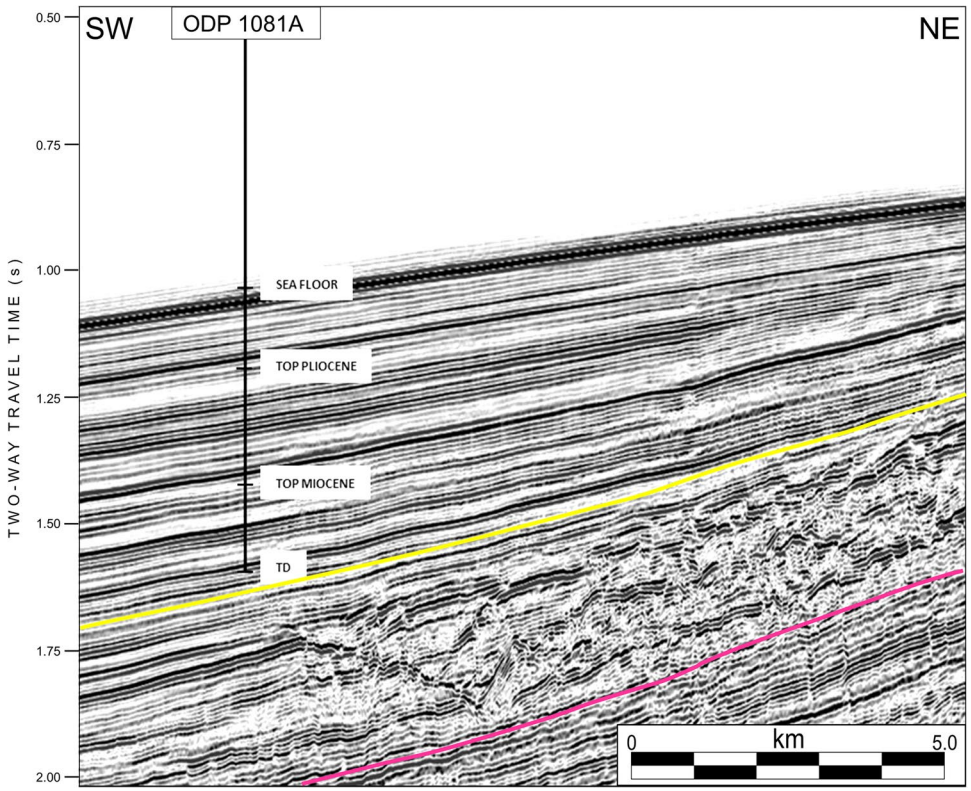

Fig. 10 Seismic profile intersecting ODP borehole 1080A showing the hole terminating above the correlative conformity of the erosion surface (yellow). Also shown is the Near Top Early Miocene horizon (magenta). Stratigraphic tops are from Wefer et al. (1998). See Footnote 1 for information on time-depth conversion. See Fig. 3 for location

Based on the oldest identified calcareous nannofossil datum (NN10), the bottom-hole date in ODP 1081A is estimated at 9.0 ± 0.2 Ma (Wefer et al. 1998). Assuming constant sedimentation rates throughout the Late Miocene and Early Pliocene of 4 cm/k.y. (Wefer et al. 1998) and extrapolating this rate linearly backwards, the time represented by the interval of 35 m below the borehole is approximately 875,000 years. Hence, the erosion surface can be assigned an age of 9.9 ± 0.2 Ma using this method. The error of ± 0.2 Ma (Wefer et al. 1998) does not however take account of possible well-to-seismic tying errors or of potential time-to-depth conversion errors. The aggregate of all these factors therefore leads to a best estimate for the minimum age of the erosion surface of 9.9 ± 1.0 Ma (i.e. Late Miocene). The eroded strata are assumed to have been pelagic and hemipelagic shales and mudstones of Miocene age (Stow 1987).

Discussion

An explanation of the processes by which a large volume of the Late Miocene outer shelf came to be excavated and re-filled must be able to account for the following key observations:

1. The external asymmetric'kidney-shaped' morphology of the excavated zone with its entirely closed perimeter.
2. The proximity to the remnant of the Phoenix High, and confinement of the depression to the outer continental shelf.
3. The internal structure including the three sub-parallel troughs each ending in a deep elliptical pit, the inwardly dipping outer margins, and the pronounced basinward curve.
4. The gross basinward plunge of the depression with a lack of any systematic base level of erosion.
5. The timing of the concurrent episodes of erosion and infill during the Late Miocene.

We considered a range of mechanisms to account for the erosional excavation of this large depression offshore Namibia, including collapse by withdrawal or removal of material from below, slumping, and current-driven erosion. The removal of underlying material by dissolution or withdrawal can cause gravity-driven collapse creating a surface depression (Bertoni and Cartwright 2006; McDonnell et al. 2007). This mechanism was considered because it is well known to be capable of forming a surface depression above the zone of underlying collapse that is characterised by an enclosed perimeter (Branney 1995; Bertoni and Cartwright 2006). It can be discounted here however, because the reflections beneath the depression are undisturbed and there are no indications of the concentric faulting or down-bending that might be expected in response to collapse (Bertoni and

Cartwright 2006). Furthermore, the absence of halite in the sediments precludes the possibility of collapse due to salt dissolution.

We also rejected the possibility that the depression is a slump scar. There is no evidence of any remnant remobilised material with a characteristic chaotic seismic facies deposited directly on the erosion surface (Frey Martinez et al. 2005; Bull et al. 2009). It is also difficult to see why a slump scar would exhibit the geometry of an enclosed perimeter with inward dipping margins. Submarine slope failure surfaces invariably plunge in a downslope direction, or ramp upwards through pre-failure stratigraphy at the toe region (Frey Martinez et al. 2005; Masson et al. 2010), neither of which is seen here. The sense of asymmetry in the long axis direction is also the opposite of what is commonly seen in slumps or rotational failures. The steepest surfaces in the erosional depression lie closest to the continental slope, but face away from it, rather than towards the downslope direction as would be the norm. There is also no trace of any remobilised material having been transported downslope from the depression to be incorporated in the age equivalent slope sediments as a mass transport complex.

The erosional depression is located close to the present-day outflow of the ephemeral Hoanib River (Fig. 1), so we considered the possibility that the feature was formed during a relative sea level lowstand as an incised valley (Posamentier 2001). However, from the palaeo-water depth reconstruction of ca. 330 m, a significant fall in relative sea level would have been required to initiate and complete the incision, and there is no evidence of such a dramatic relative sea level fall along this part of the Namibian continental margin during the Miocene (Siesser and Dingle 1981; Aizawa et al. 2000). Even more of a problem with this incised valley model, is the lack of any channel system or canyon extending basinward from the outlet of the erosional depression, which is invariably observed associated with incised valleys cut into shelf sequences elsewhere (Posamentier 2001; Bertoni and Cartwright 2006). The excavation as an incised valley fundamentally fails to explain the enclosed perimeter, the inward dipping margins of the erosion surface, and the lack of any systematic erosional base level datum. For these reasons, we reject this explanation. The only valleys that are known to exhibit U-shaped thalweg profiles are tunnel valleys, but since these only occur as a result of sub-glacial meltwater flow (Huuse and Lykke-Andersen 2000) and the nearest glaciated area at this time was in Antarctica, this possibility can also be discounted.

Bottom current activity

There are several lines of evidence pointing to the erosional depression having been formed as the result of the action of bottom currents:

1. The apparent current entry point for the depression is aligned parallel to the margin;
2. The orientation of many of the downlapping configurations of the reflections defining the internal fill also indicate a current orientation parallel to the margin;
3. Some of the reflection configurations within the infilling succession are diagnostic of contourites.

The erosive action of bottom currents on the continental slope of the Cape Basin was first recognised by Van Andel and Calvert (1971). More recently, Late Miocene slump scars observed on seismic date from the continental slope in the south of the Cape Basin have been attributed to the interaction of slope instabilities with bottom currents associated with the onset of upwelling (Weigelt and Uezelmann-Neben 2004). Further afield, a notable series of present-day km scale "erosive sub-circular depressions" has been reported from a middle slope setting in the Gulf of Cadiz with a proposed origin partly attributable to eddying within the Mediterranean Outflow Water (Garcia et al. 2016).

By contrast, examples of bottom current erosion impinging on the outermost shelf system, where slope instability is less likely to contribute to mass movements, are comparatively rare (e.g. Fulthorpe and Carter 1991; Verdicchio and Trincardi 2008). On the KwaZulu-Natal continental shelf, Green (2009) has documented the present-day role of the coast-parallel Agulhas Current in the redistribution of sediment and in relatively minor erosive activity. However, nothing comparable to the excavation geometry described in this Namibian example has previously been suggested to be linked to bottom current erosional processes. Does this imply that exceptional factors were in operation during the creation of the feature? These factors must certainly include the generation of sufficient current power to erode the substrate down to 160 m below the seabed. They must also allow for the organisation of these currents on a sufficiently long time scale in a stable position on the shelf to focus this erosional activity at the site of the excavation.

On the question of why this feature is located specifically where it is along the margin, two points can be considered. Firstly, the flow focusing effect of sea floor topography, and secondly the timing of the intensification of upwelling in the Benguela region, with the consequences for palaeo-circulation implied by that event. It is well known that current pathways can be topographically steered, even by very small-scale sea floor features (Gille et al. 2004). In order to conserve momentum, a flow may have to increase or decrease velocity in order to negotiate a topographic change. Variations in shear velocity, and hence in bed shear stress can therefore occur where fluid flow is constricted or caused to expand by changes in the topography of the sea bottom (e.g. Leeder 1999). It is conceivable therefore that the 'gap' between the positive topography of the Phoenix

High and the shoaling of water depth towards the coast may have acted as a constriction to a southward flowing bottom current. Turbulent eddies may then have been generated by the intensification of flow in the unusually large water depths of the outer shelf. This induced vorticity may then have been responsible for the erosional morphology as a kidney-shaped depression scour. The apparent direction of overall flow suggests that the southward flowing Angola Current was instrumental in the erosive process and that the ABF was situated further south than is shown in Fig. 1.

Following the above argument, we suggest that the detail of the erosional morphology of the three sub-parallel, curved troughs with three terminal deep troughs is due to the presence of instabilities within the eddies. These instabilities may have been generated by passing alongside the Phoenix High, causing division into three smaller eddies (Fig. 7b). An analogy, albeit with much larger relief, may be found in the Lesser Antilles; where large current eddies passing through gaps between the islands have been observed to break up into a number of smaller "offspring" (Simmons and Nof 2001).

We speculate that the depth and prominence of the three troughs are due to the rotating eddies coming to a relative halt close to the palaeo-self-slope break, possibly in response to a hydrographic boundary at this point (e.g. Colling et al. 2001). Having come to a halt, the three eddies then dissipated their energy by drilling down into the soft, unconsolidated substrate. Flow separation may have occurred at the edge of each developing trough, with a zone of highly disturbed flow contained within a bubble. This would have led to the current being directed downwards, with each vortex striking the surface at the reattachment point and scouring the bed (Fig. 7b; Allen 1994).

Having done their last work of erosion at the basinward end of each of the troughs, the rotating eddies could then have either lost their power or alternatively "lifted off" from contact with the sea floor if, for example, mixing with the surrounding water resulted in neutral buoyancy. This would explain the closed perimeter of the depression, the position of the deepest erosional down-cutting features, and the inwards dipping margins of the erosion surface. A similar phenomenon has been noted for the Mediterranean Outflow, where a downslope bottom current is observed to "lift off" the sea floor at a critical depth in response to the effects of relative buoyancy (Habgood et al. 2003).

It is notable that for a south-east flowing current system, the erosional depression curves to the right, i.e. in the opposite direction to the prevailing Coriolis Effect. However, a class of westward propagating mesoscale eddies, rotating counter-clockwise in the southern hemisphere, has been observed on eastern ocean boundaries (Miller et al. 2005). Hence, while overall motion seems to be in the "wrong" direction, internal deflection is consistent with the Coriolis Effect. In the type area of the northwest Pacific, these are termed Haida eddies, where they are observed to form at least once per year, with frequency rising in association with El Nino events. The eddies are 150 to 300 km in diameter and travel at speeds up to 2 cm/s, though internal rotation speeds of more than 30 cm/s, which are more than adequate to erode soft sediments, have been observed (Miller et al. 2005). Vertical extent is typically up to 1000 m (Di Lorenzo et al. 2005). Haida eddies thus offer an analogue, albeit at a somewhat larger scale, for a bottom-impinging current system that could have been responsible for erosion on the Walvis shelf.

In the southwest Atlantic, mesoscale clockwise eddies are postulated to act as a "submarine-polishing machine" on the sea floor (Viana et al. 1998). In this mechanism, the vertical downwater transference of the momentum generated by eddy rotation is strong enough to induce high bottom current velocities. These then combine with upwelling Eckman pumping, which is characteristic for cyclonic eddies, to produce a tornado-like effect along its core. In the northern South China Sea, Quaternary mesoscale eddies are identified as erosional agents on the continental slope, albeit at a subtle level (Chen et al. 2019).

In the interpretation of the seismic stratigraphy, erosion and deposition are proposed to have taken place concurrently, and this fits well within our proposed explanation of the erosional depression as having been cut by bottom currents. The mutual interaction of erosional and depositional processes is indeed widely observed in contourite systems (Rebesco et al. 2014), so accords well with our observations from the Walvis shelf. We suggest that behind the erosive frontal edge of an active bottom current, the disturbed sediment was being redeposited as downlapping clinoforms in its wake.

We postulate that the sequence of events occurred as follows:

1. Fine sediment re-suspended from the sea floor formed a benthic nepheloid layer. In deep water, this may be up to several hundred metres thick (Deuser et al. 1981).
2. Once out of the near bed region, sediment was held in suspension by the action of turbulence, which, as well as being the agent of erosion, was responsible for most of the vertical transport within the benthic boundary layer (Dade et al. 2001).
3. As the erosive eddies moved on and shear stress decreased below the settling threshold, suspended sediment began to sink back from the nepheloid layer to the near bed region. This had the effect of increasing the concentration of suspended sediment, thereby developing a density stratification, which absorbed turbulent energy.

4. In turn, this reduced shear stress and facilitated deposition of the suspended load (McCave 2004) along clinoforms behind the advancing eddies, thereby preserving a local record of the direction of movement.

In contrast, finer, slower settling particles were kept in suspension, even as shear stresses waned. In particular, deposition of aggregates of diameter < 4 μm may have been suppressed by relatively modest current speeds (McCave 2004). Some of these finer particles then came under the influence of the deep poleward current, and were transported to the south. The outcome was a fractionation process, in which silts were preferentially deposited, and finer clays kept in suspension (McCave 2004) or transported away. The initial infilling sediments are therefore predicted to be slightly coarser than their lateral neighbours in the uneroded margins of the depression. This might be expected to result in a decrease in acoustic impedance across the stratal discontinuity surface, and this would be consistent with the negative polarity of the observed reflection.

Significance of bottom current intensification at ca. 10 Ma

A causal connection may plausibly be inferred between the intensification of the Benguela Current at ca. 10 Ma as identified from DSDP and ODP studies (Siesser 1980; Diester-Haass 1990) and the erosional and depositional processes described in this paper. From their location, and from what is known of the palaeo-circulation in the region, the water mass circulation responsible for the depression and its infill was most likely to have been part of the BUS. What is less obvious is why these processes led to such profound erosional sculpting at this particular time i.e. at ca. 9.9 Ma at this location. The Phoenix High was still present as a sea floor swell, and the ABF is known to have moved up and down the coast in response to changes in the BUS, so why has such an event not occurred more than once?

It is difficult to draw conclusions as to the precise combination of factors that led to such an extraordinary erosional episode. However, it is interesting to speculate that it may have been that the initial intensification in response to glacial activity in the Antarctic resulted in a "spike" in the intensity of the Benguela Current at ca. 9.9 Ma. Subsequently, the levels of current intensity required to produce the forms observed, have not been achieved since that time.

Another possibility is that relative sea level, which had been rising on the margin more or less steadily since the Early Miocene (Siesser and Dingle 1981), reached a critical point over the study area at the same time as the Benguela Current intensified. The suggestion here is that a particular "tuning" depth occurred at just the right time, which enhanced the effects of eddy generation through the gap alongside the Phoenix High. Whatever the direct cause, the effect was a massive excavation of near sea floor sediments in a large region of the outer shelf, showing that the erosive effects of bottom currents can be intense, and highly focused, and can leave a dramatic imprint in the stratigraphic record.

Conclusions

1. The erosional depression, including its sedimentary infill, records an episode of Late Miocene bottom current intensification on the outer shelf of the Walvis Basin, and is a rare feature, with few if any obvious analogues, either locally or globally.
2. On the basis of seismic to well ties, the basinward side of the erosion surface can be dated at 9.9 ± 1.0 Ma. This constitutes a minimum age for the bottom current activity.
3. The depression coincides spatially with a low relief gap in sea floor topography next to the Phoenix High, and with the approximate location of the ABF, and it is concurrent with the intensification of the BUS at ca. 10 Ma.
4. The relative importance of these factors, and of their coincidence, is unclear, though they are postulated to have worked together in an unusual fashion to produce a "tuning" effect that resulted in the generation of mesoscale eddies associated with bottom currents sweeping south-eastwards along the shelf, parallel to the margin, and then turning sharply to the southwest into the basin.
5. The morphology of the erosion surface that defines the depression is closely related to the configuration of the reflections from the sedimentary infill, and strongly suggests that deposition occurred in the wake of the eroding eddies, and that erosion and deposition thus took place concurrently rather than sequentially.
6. The surface is thus interpreted to be diachronous, being younger at its basinward side.
7. The water depth at the time of formation of the depression was approximately 330 m.

In addition to these specific points, we draw the following general conclusions:

- Areally extensive erosion surfaces may be formed by bottom current activity on the continental shelf, though instances are rare and depend on the convergence of a specific set of conditions.
- An erosion surface such as that studied in this paper may extend over an area much greater than that covered by a typical 3D seismic survey. In such a case, incomplete coverage over an extensive erosion surface may result in it being mistaken for a (regional) sequence boundary.

Acknowledgements The authors are most grateful to NAMCOR, the National Petroleum Corporation of Namibia for granting access to seismic and borehole data. Thanks are also due to Schlumberger for the donation of Geoframe software and to IHS Markit for the donation of Kingdom software. The manuscript was greatly improved by comments from an anonymous reviewer and from Roger Swart. AH was partly funded by the American Association of Petroleum Geologists for work which included this study.

Funding AH received a one off Grant-in Aid from the American Association for Petroleum Geology for work which included this study.

Data availability Seismic and well data are owned by Namcor, the National Petroleum Corporation of Namibia; DSDP and ODP data are open access.

Code availability Not applicable.

Declarations

Consent to participate Not applicable.

Consent for publication Namcor—pending.

Conflict of interest The authors declare no competing interests.

References

Abreu V, Sullivan M, Pirmez C, Mohrig D (2003) Lateral accretion packages (LAPs): an important reservoir element in deep water sinuous channels. Mar Pet Geol 20:631–648

Aizawa M, Bluck B, Cartwright J, Milner S, Swart R, Ward J (2000) Constraints on the geomorphological evolution of Namibia from the offshore stratigraphic record. Geol Surv Namibia Comm 12:337–346

Allen J (1994) Fundamental properties of fluids, their relation to sediment transport processes In: Pye K (ed), Sediment transport, depositional processes. Blackwell Sci Publ Oxford 2:25–60

Ashcroft W (2011) A petroleum geologist's guide to seismic reflection. John Wiley & Sons, Chichester, UK, p 176

Bertoni C, Cartwright J (2006) Controls on the basinwide architecture of the Messinian evaporites on the Levant margin, Eastern Mediterranean. Sed Geol 188–189:93–114

Branney M (1995) Downsag, extension at calderas: new perspectives on collapse geometries from ice-melt, mining, volcanic subsidence. Bull Volcanol 57:303–318

Brown L, Fisher W (1977) Seismic-stratigraphic interpretation of depositional systems: examples from brazilian rift and pull-apart basins: section 2 application of seismic reflection configuration to stratigraphic interpretation. In: Payton (ed) Seismic stratigraphy-applications to hydrocarbon exploration, AAPG Memoir 26:213–248

Bull S, Cartwright J, Huuse, M (2009) A review of kinematic indicators from mass-transport complexes using 3D seismic data Marine and Petroleum Geology 26:1132–1151

Cartwright J, Santamarina C (2015) Seismic characteristics of fluid escape pipes in sedimentary basins: implications for pipe genesis. Mar Pet Geol 65:126–140

Catuneanu O (2003) Sequence Stratigraphy of Clastic Systems. Geological Association of Canada 16:1–248

Chen H, Zhang W, Xiea X, Ren J (2019) Sediment dynamics driven by contour currents, mesoscale eddies along continental slope: acase study of the northern South China Sea. Mar Geol 409:48–66

Clement A, Gordon A (1995) The absolute velocity field of Agulhas eddies and the Benguela Current. J Geophys Res 100 Cll 22:591–22,601

Colling A, Open University Course Team (2001) Ocean Circulation. Butterworth-Heinemann. 286pp

Corner B, Cartwright J, Swart R (2002) Volcanic passive margin of Namibia: a potential fields perspective In: Menzies, M, et al (eds), Volcanic Rifted margins. Geol Soc Am Spec Paper 362:203–220

Dade W, Hogg A, Boudreau B (2001) Physics of flow above the sediment–water interface. In: Boudreau B, Jorgensen B (eds) The Benthic Boundary Layer. Oxford Univ Press, New York, pp 4–43

Deuser W, Ross E, Anderson R (1981) Seasonality in the supply of sediment to the deep Sargasso Sea, implications for the rapid transfer of matter to the deep ocean. Deep-Sea Res 28:495–505

Di Lorenzo E, Foreman M, Crawford W (2005) Modelling the generation of Haida Eddies. Deep Sea Research II 52:853–873

Diester-Haass L, Meyers P, Rothe P (1990) Miocene history of the Benguela Current and Antarctic ice volumes; evidence from rhythmic sedimentation and current growth across the Walvis Ridge (Deep Sea Drilling Project Sites 362, 532). Paleoceanography 5:685–707. https://doi.org/10.1029/PA005i005p00685

Emery D, Myers K (eds) (1996) Sequence Stratigraphy. Blackwell Science, Oxford, p 297

Frey Martinez J, Cartwright J, Hall B (2005) 3D seismic interpretation of slump complexes: examples from the continental margin of Israel. Basin Res 17(1):83–108

Fulthorpe C, Carter R (1991) Continental shelf progradation by sediment drift accretion. Geol Soc Am Bull 103(2):300–309

Garcia M, Hernández-Molina F, Alonso B, Vázquez J, Ercilla G, Llave E, Casas D (2016) Erosive sub-circular depressions on the Guadalquivir Bank (Gulf of Cadiz): interaction between bottom current, mass-wasting and tectonic processes. Mar Geol 378:5–19

Gille S, Metzger E, Tokmakian R (2004) Seafloor topography and ocean circulation. Oceanography 17:47–54

Gornitz V (2009) Sea level change, post-glacial. In: Gornitz (ed) Encyclopedia of Paleoclimatology and Ancient Environments. Encyclopedia of Earth Sciences Series. Springer:887–893

Green A (2009) Sediment dynamics on the narrow, canyon-incised and current-swept shelf of the northern KwaZulu-Natal continental shelf, South Africa. Geo-Mar Lett 29:201–219

Habgood E, Kenyon N, Masson D, Akhmetzhanov A, Weaver P, Gardner J, Mulder T (2003) Deep-water sediment wave fields, bottom current sand channels and gravity flow channel-lobe systems: Gulf of Cadiz, NE Atlantic. Sedimentology 50:483–510

Hall S, Bird D, McLean D, Towle P, Grant J, Danque H (2018) New constraints on the age of the opening of the South Atlantic basin. Mar Pet Geol 95:50–66

Heine C, Zoethout J, Műller R (2013) Kinematics of the South Atlantic rift. Solid Earth 4:215–253

Holtar E, Forsberg A (2000) Postrift development of the Walvis Basin, Namibia: rsults from the exploration campaign in Quadrant 1911. In: Mello M, Katz B (eds), Petroleum Systems of South Atlantic Margins. AAPG Memoir 73 429–446

Huuse M, Lykke-Andersen H (2000) Overdeepened Quaternary valleys in the eastern Danish North Sea: morphology and origin. Quatern Sci Rev 19:1233–1253

Jackson M, Hudec M, Hegarty K (2005) The Great West African Tertiary coastal uplift: fact or fiction? A perspective from the Angolan divergent margin. Tectonics 24:TC6014, 101029/2005TC001836

Jansen J, Ufkes E, Schneider R (1996) Late Quaternary movements of the Angola-Benguela Front, SE Atlantic, and implications for advection in the Equatorial Ocean. In: Webb D (ed) Wefer G,

Berger W Siedler G. The South Atlantic: Present and Past Circulation. Springer-Verlag, Berlin Heidelberg, pp 553–575
Lass H, Schmidt M, Mohrholz V, Nausch G (2000) Hydrographic and current measurements in the area of the Angola-Benguela front. J Phys Oceanogr 30:2589–2609
Leeder M (1999) Sedimentology, sedimentary basins: from turbulence to tectonics. Blackwell Science, Oxford, p 608
Light M, Maslanyj M, Greenwood R, Banks N (1993) Seismic sequence stratigraphy and tectonics offshore Namibia. In: Williams G, Dobb A (eds) Tectonics and seismic sequence stratigraphy. Geol Soc Spec Publ 71:163–191.
Masson D, Plets R, Huvenne V, Wynne R, Bett B (2010) Sedimentology and depositional history of Holocene sandy contourites on the lower slope of the Faroe-Shetland Channel, northwest of the UK. Mar Geol 268:85–6
McCave I (2004) Size sorting during transport, deposition of fine sediments: sortable silt, flow speed In: Rebesco, M, Camerlenghi, A (eds) Contourites: developments in Sedimentology 60 Elsevier 121–142
McDonnell A, Loucks R, Dooley T (2007) Quantifying the origin and geometry of circular sag structures in northern Fort Worth Basin, Texas: paleocave collapse, pull-apart fault systems, or hydrothermal alteration? AAPG Bull 91(9):1295–1318
Miller L, Robert M, Crawford W (2005) Editorial: the large, westward-propagating Haida Eddies of the Pacific eastern boundary Deep Sea Res II 52:845–851
Mitchum R, Vail P, Sangree J (1977) Seismic stratigraphy and global changes of sea level. Part 6, Stratigraphic interpretation of seismic reflection patterns in depositional sequences. AAPG Mem 26:117–133
Penduff T, Barnier B, Beranger K, Verron J (2001) Comparison of near-surface mean, eddy flows from two numerical models of the South Atlantic Ocean J Geophys Res v106, C8, p16,857–16,867
Pérez-Díaz L, Eagles L (2014) Constraining South Atlantic growth with seafloor spreading data. Tectonics 33:1848–1873, 101002/2014TC003644
Posamentier H (2001) Lowstand alluvial bypass systems: Incised vs unincised. AAPG Bull 85(10):1771–1793
Pufahl P, Maslin M, Anderson L, Brüchert V, Jansen F, Lin H, Perez M, Vidal L, Shipboard Scientific Party (1998) Lithostratigraphic summary for Leg 175: Angola-Benguela upwelling system In: Wefer, G, Berger W, Richter C, et al Proc ODP Init Repts 175: College Station TX (Ocean Drilling Program) 533–542 https://doi.org/10.2973/odp.proc.ir.175.118.1998
Rebesco M, Hernandez-Molina F, Van Rooij D, Wahlin A (2014) Contourites, associated sediments controlled by deep-water circulation processes: state-of-the-art, future Considerations. Mar Geol 352:111–154
Rommerskirchen F, Condon T, Mollenhauer G, Dupont L (2011) Miocene to Pliocene development of surface and subsurface temperatures in the Benguela Current system. Paleoceanography, 26:PA3216 101029/2010PA002074
Schumm S (1993) River response to base level change: Implications for sequence stratigraphy. J Geol 101:279–294
Shannon L (1985) The Benguela ecosystem: Part I Evolution of the Benguela, physical features and processes. Oceanogr Mar Biol 23:105–182
Sheriff R (1977) Limitations on resolution of seismic reflections and geologic detail derivable from them. In: Payton, C (ed), Seismic Stratigraphy — Applications to Hydrocarbon Exploration. Memoir 26 AAPG Tulsa Oklahoma 3–14
Siesser W (1980) Late Miocene origin of the Benguela upwelling system off northern Namibia. Science 208:283–285. https://doi.org/10.1126/science.208.4441.283
Siesser W, Dingle R (1981) Tertiary sea-level movements around Southern Africa. J Geol 89:83–96
Simmons H, Nof D (2001) The squeezing of eddies through gaps. J Phys Ocean 32:314–335
Stewart S (2003) How will we recognize buried impact craters in terrestrial sedimentary basins? Geology 31:929–932
Stow D (1987) South Atlantic organic-rich sediments: facies, processes and environments of deposition. In: Brooks J, Fleet A (eds) Marine Petroleum Source Rocks. Geol Soc London Spec Publ 26:287–299
Vail P, Mitchum R, Todd R, Widmier J, Thomson S, Sangree J, Bubb J, Hatleid W (1977) Seismic stratigraphy and global changes of sea level. In: Payton, C (ed), Seismic stratigraphy - applications to hydrocarbon exploration. Memoir 26 AAPG Tulsa Oklahoma 49–212
Verdicchio G, Trincardi F (2008) Mediterranean shelf-edge muddy contourites: examples from the Gela and South Adriatic basins. Geo-Mar Lett 28:137–151
Viana A, Faugeres J, Kowsmann R, Lima J, Caddah L, Rizzo J (1998) Hydrology, morphology and sedimentology of the Campos continental margin, offshore Brazil. Sed Geol 115:133–157
Van Andel T, Calvert S (1971) Evolution of sediment wedge, Walvis shelf, southwest Africa. J Geol 79:585–602
Ward J, Corbett I (1990) Towards an age for the Namib. In: Seely, M (ed), Namib ecology: 25 years of Namib research Transvaal Museum Monograph 7, Pretoria 17–26
Wefer G, Berger W, Richter C, et al. (eds) (1998) Proc ODP, Initial Reports, 175 Ocean Drilling Program, College Station, Texas https://doi.org/10.2973/odp.proc.ir.175.1998
Weigelt E, Uenzelmann-Neben G (2004) Sediment deposits in the Cape Basin: indications for shifting ocean currents? AAPG Bull 88(6):765–780
Wonham J, Jayr S, Mougamba R, Chuilon P (2000) 3D sedimentary evolution of a canyon fill (Lower Miocene-age) from the Mandorove Formation, offshore Gabon. Mar Petrol Geol 17:175–197